

General Model for the Nonlinear pH Dynamics in the Oxidation of Sulfur(−II) Species

C. Wayland Rushing and Richard C. Thompson*

Department of Chemistry, University of Missouri-Columbia, Columbia, Missouri 65211

Qingyu Gao†

Department of Energy Utilization and Chemical Engineering, China University of Mining and Technology, Xuzhou, 221008 P. R. China

Received: June 30, 2000; In Final Form: September 20, 2000

A general kinetic feature has been observed experimentally for the oxidation of the sulfur(−II) species thiosulfate, thiourea, thiocyanate, and sulfide by chlorite and other multi-equivalent oxidants under appropriate, unbuffered batch conditions. This “fingerprint” consists of an initial rise in pH followed by an autocatalytic drop in pH or oligo-oscillatory behavior. These systems also exhibit oscillations and other complex dynamical behavior in a continuous-flow stirred tank reactor (CSTR). The previously proposed general models that are oxidant based do not successfully explain the observed pH effects. We propose a simple, general model that is based upon the changing oxidation states of sulfur to explain the general pH features. The scheme qualitatively models autocatalysis and oligo-oscillations in batch and simple and complex oscillations in a CSTR. The general model consists of three separate stages: negative hydrogen ion feedback (S(−II) to S(0)), a transition of S(0) to S(IV), and positive proton feedback from S(IV) to S(VI).

Introduction

The first of the chlorite-driven oscillators was discovered in 1981.¹ Since then, the number of known oscillators based upon chlorite have grown to include a wide variety of chemical systems. They require the presence of another halogen-containing species, with the notable exception of a subfamily in which the reductant is a S(−II) species: thiosulfate,² sulfide,³ thiocyanate,⁴ and thiourea.⁵ These S(−II) systems exhibit some of the most complex dynamical behavior of any of the chlorite oscillators.

Although considerable progress has been made in understanding the mechanistic details of chlorite-based oscillators, a number of issues remain. While some specific systems have been successfully modeled, the most notable being the chlorite–iodide system,^{6–8} most are still awaiting explanation. Rábai and Orbán have suggested a general model for the chlorite-based oscillators in an attempt to explain the general nonlinear behavior observed.⁹ While their model is in many respects quite successful, it does have several limitations. The most notable is no provision for pH dynamics which prevents it from accurately describing the nonlinear behavior that is observed during the oxidation of sulfur(−II) species.

We noted that the literature provides a number of examples of nonlinear pH kinetic profiles during the oxidation of several sulfur(−II) species by not only chlorite¹⁰ but also hydrogen peroxide,^{11–16} iodate,¹⁷ periodate,¹⁸ and peroxodisulfate.¹⁹ All of these systems have similar pH kinetic profiles—an initial rise in pH followed by an autocatalytic or oligo-oscillatory drop. If sulfur is a main driving force in the nonlinear behavior then we would expect to see the same features in other multi-equivalent oxidant-S(−II) systems. To this end, we have

reinvestigated the pH effects observed during the oxidation of several sulfur(−II) species by chlorite and hydrogen peroxide. Under appropriate, unbuffered batch conditions all the systems that were investigated have the same general features as those previously reported.

Due to the similarities of the various systems we believe that the chemistry of the sulfur species is a main driving force for the nonlinear behavior observed in these systems. We therefore propose a simple, general model based upon changes in the oxidation state of sulfur in the presence of a generic oxidant. The proposed model is not meant to explain the experimental findings of any individual system, as this would require a more detailed mechanism. We only considered general reactions that would be common among all the systems. The proposed model successfully simulates the general pH features that are experimentally observed in batch and predicts pH oscillations in a continuous-flow stirred tank reactor (CSTR).

Experimental Section

Materials. Reagent grade H₂SO₄, KSCN, Na₂S, Na₂S₂O₃, H₂O₂, and NaOH were used without further purification. NaClO₂ obtained from Aldrich (≈80%) was recrystallized twice from 80% ethanol–water in the range 25 to −20 °C resulting in a purity >99% determined by iodometric titration.²⁰ Thiourea was used as received or was recrystallized twice. Purified DTPMP (diethylenetriaminepentamethylenephosphonic acid) and EDTMP (ethylenediaminetetramethylenephosphonic acid) were obtained from Dow Chemical. Sodium sulfide solutions were assayed iodometrically every 2 days. H₂O₂ was standardized with permanganate every day. All solutions were prepared in triply distilled water (with the last distillation from basic permanganate).

The batch reactions were carried out in a thermostated Plexiglas reactor with a volume of 42–45 mL. All reactant

* Corresponding author. Fax: (573) 882-2754. E-mail: thompsonr@missouri.edu.

† E-mail: gaoyu1@public.xz.js.cn.

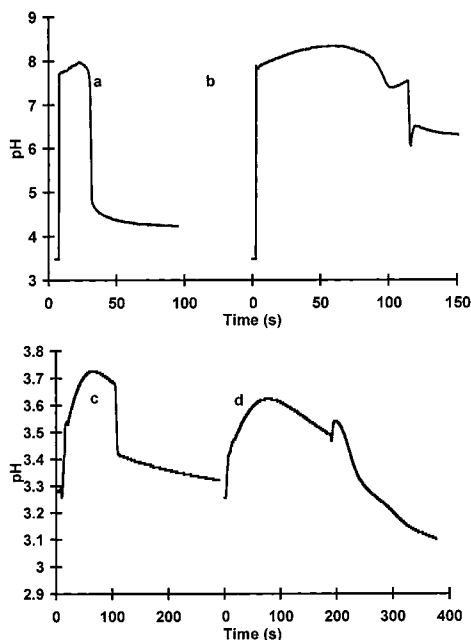


Figure 1. Measured pH vs time curves for the chlorite–sulfide (a and b) and chlorite–thiourea (c and d) systems. Chlorite–sulfide: $[\text{H}^+]_0 = 3.28 \times 10^{-4} \text{ M}$; $[\text{S}^{2-}]_0 = 7.25 \times 10^{-4} \text{ M}$; $[\text{ClO}_2^-] = 6.13 \times 10^{-3} \text{ M}$ (a), $6.03 \times 10^{-3} \text{ M}$ (b). Chlorite–thiourea; $[\text{H}^+]_0 = 6.00 \times 10^{-4} \text{ M}$; $[\text{thiourea}]_0 = 9.00 \times 10^{-4} \text{ M}$; $[\text{ClO}_2^-] = 3.00 \times 10^{-3} \text{ M}$ (c), $2.00 \times 10^{-3} \text{ M}$ (d).

solutions were deaerated by passing a nitrogen stream through the solutions for 10 min. The reactions were initiated by addition of the S(–II) species. To prevent air interference during the reaction a small layer of N_2 was kept above the solution. The pH and potential were followed with a glass and platinum electrode, respectively, utilizing a double junction ISE reference electrode.

The bulk of the batch experiments were concerned with finding the appropriate conditions in which the general fingerprint of the sulfur(–II) systems was present. For the hydrogen peroxide systems previous studies allowed for a rapid determination of the necessary conditions. However, previous studies of the chlorite systems provided little hint of the appropriate conditions since they generally used buffered or highly acidic media. Our methodology involved a systematic variation of the reactant concentrations until the general kinetic feature was observed. It was found that the fingerprint is present only under a very narrow range of experimental conditions, but was found in each S(–II) system examined.

Results

Batch Experiments. Buffers or highly acidic conditions were used in most of the previous studies of the chlorite–sulfur(–II) batch reactions. We investigated the pH effects in the chlorite oxidation of sulfide, thiourea, thiosulfate, and thiocyanate and the H_2O_2 oxidation of the thiosulfate and thiocyanate under unbuffered batch conditions.

Figure 1 displays the general kinetic features observed in the chlorite–sulfide and chlorite–thiourea reactions under appropriate conditions. Similar results were obtained for the chlorite–thiosulfate, chlorite–thiocyanate, hydrogen peroxide–thiosulfate, and hydrogen peroxide–thiocyanate systems. There is an initial rise in pH followed by an autocatalytic or oligo-oscillatory drop. The initial rise is either monophasic, as in the sulfide system (the large, instantaneous rise in pH is due to addition of

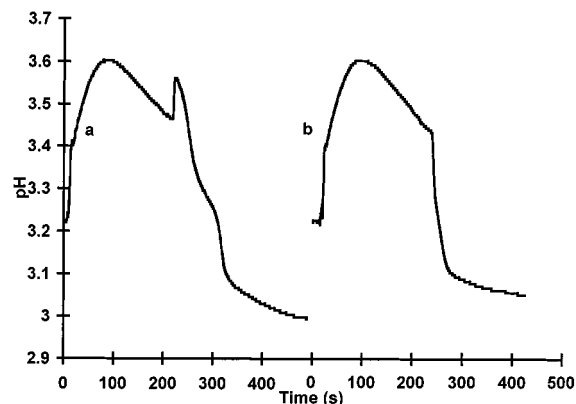


Figure 2. Chlorite–thiourea batch reactions when left in contact with air (a) and when protected (b). $[\text{H}^+]_0 = 6.00 \times 10^{-4} \text{ M}$; $[\text{thiourea}]_0 = 9.00 \times 10^{-4} \text{ M}$; $[\text{ClO}_2^-]_0 = 2.50 \times 10^{-3} \text{ M}$.

the basic sulfide solution), or biphasic, as in the thiourea system. The change in pH is accompanied by a very similar change in potential (Figure 1S). A monophasic or biphasic rise in potential is followed by an autocatalytic rise. This general feature of pH and potential change is not unique to the chlorite and hydrogen peroxide systems, but has also been observed under appropriate conditions with a number of additional multi-equivalent oxidants.^{10,13–19} This feature can therefore be thought of as a “fingerprint” for nonlinear behavior arising from the sulfur(–II) chemistry.

Nagypál and Epstein have reported very poor reproducibility in their investigation of the ClO_2^- and $\text{S}_2\text{O}_3^{2-}$ clock reaction.²¹ They found that for “identical” reaction conditions the reaction took from a matter of seconds to a couple of hours to reach completion. We apparently avoided this difficulty by using significantly lower reactant concentrations; the system showed very good reproducibility under a wide variety of conditions.

An important feature of these systems is whether the reactions are exposed to air. Figure 2 illustrates the behavior observed for the chlorite–thiourea system when the reactions were performed in the presence of air and under nitrogen. These systems are very air sensitive and yielded reproducible results only when protected from air. (All of the experiments in Figure 1 were performed nitrogen. Under these conditions the oligo-oscillatory behavior observed is not present until the oxidant concentration is below $2.30 \times 10^{-3} \text{ M}$. But if exposed to air it occurs at higher oxidant concentrations as seen in Figure 2.)

Many of the sulfur(–II) systems have previously been shown to be catalyzed by copper ions.^{12–15,19} Studies of the oxidation of sulfur(–II) species are often done with added copper(II) in order to obtain nonlinear behavior. Doona and Stanbury have shown that traces of Cu(II) can dramatically catalyze the oxidation of thiourea by $[\text{IrCl}_6]^{2-}$, ClO_2^- , IO_3^- , BrO_3^- , and ClO_2 .²² We tested for trace metal ion catalysis in our systems in several ways. First, results obtained with commercially available thiourea were compared to those with twice-recrystallized thiourea. Both reactions were repeated with $6 \mu\text{M}$ DTPMP and EDTMP (1% of total sulfur concentration); these chelators have been shown to effectively sequester many trace metal ions.²³ These chelators were also added to the sulfide systems. No appreciable difference in any of the traces was observed.

Model. We propose the general model summarized in Table 1 to simulate the pH dynamics associated with the oxidation of sulfur(–II) species. To make the model as general as possible, no acid–base equilibria of the oxidant or reductant are taken into account. No distinction is made among the chemical species

TABLE 1: Reactions of the General Model for the Sulfur(−II) Systems

no.	reactions
(1)	$\text{OX} + \text{S}(-\text{II}) \rightarrow \text{S}(0) + \text{OH}^-$
(2)	$\text{S}(0) + \text{S}(-\text{II}) \rightarrow \text{S}(-\text{I})^a + \text{OH}^-$
(3)	$\text{S}(-1) + \text{OX} \rightarrow 2\text{S}(0)$
(4)	$\text{S}(-1) + \text{OX} + \text{OH}^- \rightarrow 2\text{S}(0) + \text{OH}^-$
(5)	$\text{S}(0) + \text{OX} \rightarrow \text{S}(\text{II})$
(6)	$\text{S}(0) + \text{OX} + \text{OH}^- \rightarrow \text{S}(\text{II}) + \text{OH}^-$
(7)	$\text{S}(\text{II}) + \text{OX} \rightarrow \text{HSO}_3^- + \text{H}^+$
(8)	$\text{HSO}_3^- + \text{OX} \rightarrow \text{SO}_4^{2-} + \text{H}^+$
(9)	$\text{HSO}_3^- + \text{OX} + \text{H}^+ \rightarrow \text{SO}_4^{2-} + 2\text{H}^+$
(10)	$\text{SO}_3^{2-} + \text{OX} \rightarrow \text{SO}_4^{2-}$
(11)	$\text{HSO}_3^- \rightarrow \text{SO}_3^{2-} + \text{H}^+$
(12)	$\text{SO}_3^{2-} + \text{H}^+ \rightarrow \text{HSO}_3^-$
(13)	$\text{H}_2\text{O} \rightarrow \text{H}^+ + \text{OH}^-$
(14)	$\text{H}^+ + \text{OH}^- \rightarrow \text{H}_2\text{O}$

^a S(−1) represents a disulfide.

that could predominate at sulfur oxidation states less than +4. (The sulfur(−II) species in the model can be related to the specific species HS^- , $\text{S}_2\text{O}_3^{2-}$, SCN^- , and $(\text{NH}_2)_2\text{CS}$. The sulfur(−1) species would likely be S_2^{2-} , $\text{O}_3\text{S}-\text{S}^-\text{S}-\text{SO}_3^{2-}$, or $(\text{SCN})_2$ while sulfur(0) could be $1/8 \text{S}_8$, HOSH , $\text{HOS}-\text{SO}_3^-$, or HOSCN . In our model we propose the S(II) intermediate. However, in many of the specific systems the S(0) species is taken directly to SO_3^{2-} by 2 equivalents of oxidant. For a more detailed explanation of the proposed models for the specific systems see refs 10, 19, 33, and 34.) The inclusion of specific species for S(IV) and S(VI) is necessary for the success of the model. Any nonlinear behavior arising from the chemistry of the oxidant is omitted from this model to emphasize that arising from the changing oxidation states of sulfur.

Many of the oscillatory systems that involve the oxidation of S(−II) can be described as “pH-driven” oscillators. Therefore, there must be both positive and negative hydrogen ion feedback, with one of them also being autocatalytic in nature. The model can be broken down into three constituent parts: negative hydrogen ion feedback, positive hydrogen feedback, and transition reactions.

Reactions 1 and 2 provide the negative hydrogen ion feedback and account for the initial rise in pH that is observed under batch conditions. Reactions 8 and 9, the oxidation of bisulfite to sulfate, provide positive proton feedback with reaction 9 also being autocatalytic in hydrogen ion. Reactions 3–7 are transition reactions allowing for the conversion of S(−1) \rightarrow S(IV) and reactions 11–14 are protonation equilibria. Reactions 4 and 6 have previously been proposed in thiosulfate and thiocyanate reactions and are necessary for oscillations to occur in a CSTR.^{14,15,16}

Reported rate constants when $\text{OX} = \text{H}_2\text{O}_2$ were used for reactions 8–10 as a starting point.^{24,25} Values for $k_1 - k_7$ were assigned mainly by trial and error while attempting to fit the general features and oligo-oscillatory behavior that was found under batch conditions. For successful modeling a number of constraints were needed. First, there needed to be effective competition for the sulfur(0) intermediate by the sulfur(−II) species and the oxidant, with the sulfur(0)–sulfur(−II) reaction predominating under acidic conditions and the sulfur(0)–oxidant reaction predominating under basic conditions. Second, the autocatalytic formation of the sulfur(0) intermediate by reactions 2–4 is necessary for oligo-oscillatory behavior. Any detailed mechanism for specific oxidant and S(−II) species would be far more complex than the simple model presented. It is important to note that the proposed model is a minimal oscillator under open conditions.

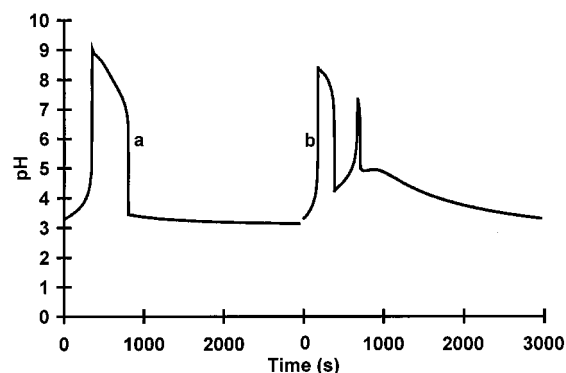


Figure 3. Batch simulation of the general model. $[\text{H}^+]_0 = 5.00 \times 10^{-4} \text{ M}$; $[\text{S}(-\text{II})]_0 = 4.00 \times 10^{-3} \text{ M}$; $[\text{OX}]_0 = 1.00 \times 10^{-2} \text{ M}$ (a), $2.10 \times 10^{-2} \text{ M}$ (b).

TABLE 2: Rate Equations and Rate Constants for the General Model

rate equations	rate constants at 25°
$R_1 = k_1[\text{OX}][\text{S}(-\text{II})]$	$k_1 = 0.021 \text{ M}^{-1} \text{ s}^{-1}$
$R_2 = k_2[\text{S}(0)][\text{S}(-\text{II})]$	$k_2 = 50 \text{ M}^{-1} \text{ s}^{-1}$
$R_3 = k_3[\text{S}(-1)][\text{OX}]$	$k_3 = 0.01 \text{ M}^{-1} \text{ s}^{-1}$
$R_4 = k_4[\text{S}(-1)][\text{OX}][\text{OH}^-]$	$k_4 = 8.0 \times 10^5 \text{ M}^{-2} \text{ s}^{-1}$
$R_5 = k_5[\text{S}(0)][\text{OX}]$	$k_5 = 1.0 \text{ M}^{-1} \text{ s}^{-1}$
$R_6 = k_6[\text{S}(0)][\text{OX}][\text{OH}^-]$	$k_6 = 1.2 \times 10^6 \text{ M}^{-2} \text{ s}^{-1}$
$R_7 = k_7[\text{S}(\text{II})][\text{OX}]$	$k_7 = 1.0 \times 10^{11} \text{ M}^{-1} \text{ s}^{-1}$
$R_8 = k_8[\text{HSO}_3^-][\text{OX}]$	$k_8 = 7.0 \text{ M}^{-1} \text{ s}^{-1}$
$R_9 = k_9[\text{HSO}_3^-][\text{OX}][\text{H}^+]$	$k_9 = 1.48 \times 10^7 \text{ M}^{-2} \text{ s}^{-1}$
$R_{10} = k_{10}[\text{SO}_3^{2-}][\text{OX}]$	$k_{10} = 0.2 \text{ M}^{-1} \text{ s}^{-1}$
$R_{11} = k_{11}[\text{HSO}_3^-]$	$k_{11} = 3.0 \times 10^3 \text{ s}^{-1}$
$R_{12} = k_{12}[\text{SO}_3^{2-}][\text{H}^+]$	$k_{12} = 5.0 \times 10^{10} \text{ M}^{-1} \text{ s}^{-1}$
$R_{13} = k_{13}[\text{H}_2\text{O}]$	$k_{13}[\text{H}_2\text{O}] = 1.0 \times 10^{-3} \text{ M s}^{-1}$
$R_{14} = k_{14}[\text{H}^+][\text{OH}^-]$	$k_{14} = 1.0 \times 10^{11} \text{ M}^{-1} \text{ s}^{-1}$

Discussion

The numerical integrations of the rate equations shown in Table 2 were carried out using a semi-implicit Runge–Kutta method²⁶ utilizing the program SIMULATE.²⁷ To check the results of the Runge–Kutta method, selected experiments were also simulated using the Gear²⁸ algorithm and the program GEPASI,²⁹ which utilizes the LSODE integrator.³⁰ There was no difference in the results obtained by the different methods.

To test the validity of the proposed model we set out to simulate several general features of the sulfur systems. As we are going to show, the model can qualitatively simulate nearly all of the behavior observed experimentally in the various systems. The model is capable of simulating the general behavior seen in batch; a general rise in pH followed by an autocatalytic drop in pH (Figure 3, trace a). The more complex phenomena of oligo-oscillations in batch can also be successfully modeled (Figure 3, trace b). The resulting simulations not only agree well with the experimental results of this paper but also with many of those previously reported.^{10,13–19} Interestingly, the general model gives very similar results to the model developed by Kurin-Csörgei et al. for the hydrogen peroxide–thiosulfate system.¹⁴

In several of the S(−II) systems the initial rise in pH is biphasic (Figure 1, traces c and d). However, the general model is not capable of simulating this behavior. Shortening the model by omitting reactions 4 and 6 allows simulation of the two separate rises in pH (Figure 2S). Reactions 4 and 6 allow for a too rapid a conversion of S(−I) to S(II). This would have the effect of allowing the acid producing reactions, 7–9, to predominate early and obscure the second rise. Unfortunately, the shortened model is incapable of producing either oligo-oscillations in batch or oscillations in a CSTR.

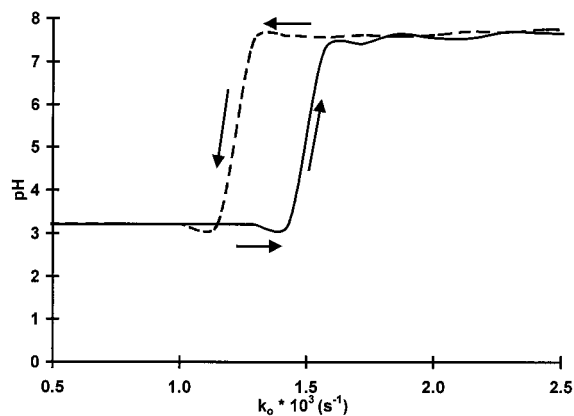


Figure 4. Simulated bi-stability. Hysteresis between a low-pH and a high-pH steady state as the flow rate is varied in both directions. $[H^+]_o = 5.00 \times 10^{-4}$ M.; $[S(-II)]_o = 4.00 \times 10^{-4}$ M.; $[ClO_2^-]_o = 0.02$ M.

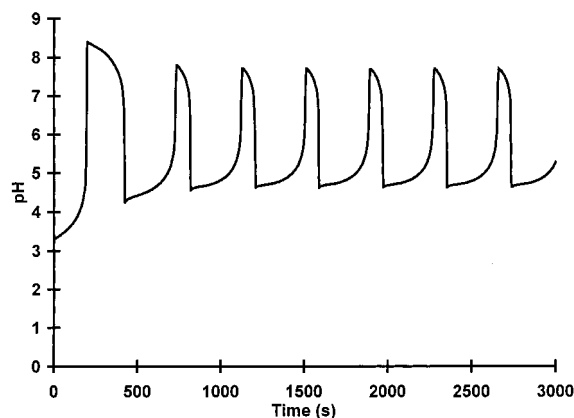


Figure 5. Simulated simple oscillations in a CSTR. $[H^+]_o = 5.00 \times 10^{-4}$ M.; $[S(-II)]_o = 4.00 \times 10^{-4}$ M.; $[OX]_o = 0.02$ M.; $k_o = 4.00 \times 10^{-4}$ s $^{-1}$.

An important feature in nonlinear systems is bi-stability. The S(-II) systems exhibit bi-stability between two stationary states associated with low and high pH values. The simulated bi-stability, i.e., the hysteresis between the two steady states as the flow is varied, is shown in Figure 4. However, the range of input concentrations and flow rates where bi-stability occurs is much narrower than the experimentally derived hysteresis plots. This is not of great concern as the shape of the hysteresis plot is very dependent upon the rate constants and would vary depending on the particular system being investigated.

Simple pH oscillations calculated with this model under flow conditions are shown in Figure 5. The shape and other characteristics of the oscillations are sensitive to the adjustable rate constants. Interestingly, the model is capable of simulating oscillations not only in the CSTR but also under batch conditions as seen in Figure 6. Batch oscillations in potential have previously been observed in S(-II) systems.³¹ Since these experiments were done under buffered conditions no pH oscillations were observed. However the model does suggest the possibility that some S(-II) systems might have the capability for pH oscillations under batch conditions.

Many of the S(-II) systems not only exhibit simple oscillations but also complex oscillations and chaos.^{5,13-15} At low flow rate the system exhibits simple oscillations as discussed earlier. As the flow rate is increased, a second oscillatory peak begins to emerge after the initial large peak (Figure 3S) resulting in period 2 oscillations (Figure 7). Unfortunately the model is incapable of simulating chaos or other more complex phenom-

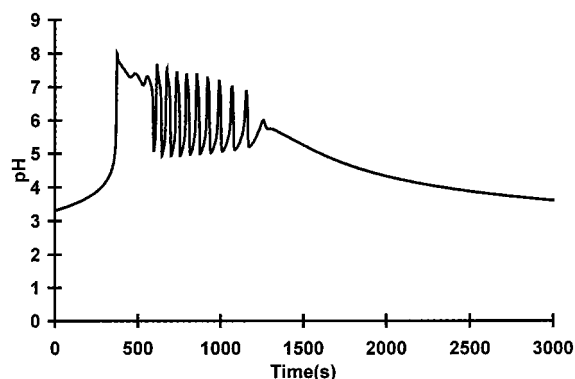


Figure 6. Simulated batch oscillations. $[H^+]_o = 5.00 \times 10^{-4}$ M.; $[S(-II)]_o = 4.00 \times 10^{-3}$ M.; $[OX]_o = 0.02$ M.

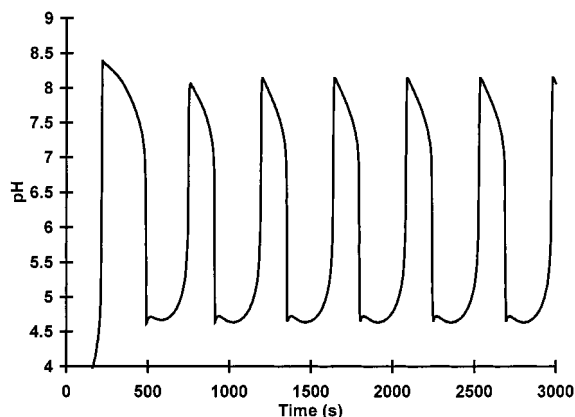


Figure 7. Simulated complex oscillations in a CSTR. $[H^+]_o = 5.00 \times 10^{-4}$ M.; $[S(-II)]_o = 4.00 \times 10^{-3}$ M.; $[OX]_o = 0.02$ M.; $k_o = 1.20 \times 10^{-3}$ s $^{-1}$.

ena. As the flow rate is increased further, the model no longer gives oscillations but yields the high pH steady state.

The most exotic and complex behavior observed in the sulfur(-II) systems occurs when chlorite is the oxidant.^{5,32} The chlorite-based model proposed by Rábai and Orbán successfully demonstrates that nonlinear behavior can arise from the oxidant chemistry only.⁹ One can envision that in systems that involve not only a sulfur(-II) species but also chlorite there are two nonlinear driving forces which could lead to the exotic phenomena that are observed.

There have been great strides in the development of general models for chemical oscillators. In most of these models the systems are thought of as being oxidant driven, i.e., bromate and chlorite systems. However, these models are not successful in portraying the complex pH effects that are associated with the nonlinear oxidation of sulfur(-II) species. This is mainly due to the complex chemistry that S(-II) species can undergo and the variety of intermediate oxidation states that can be formed. The model proposed here is the first that is substrate based. Comparison of the calculated results and the known chemical systems suggests to us that our model can serve as a guide in many of the chemical systems involving oxidation of S(-II). The model successfully simulates the qualitative behavior that is seen in many of the experimental systems. The general model that is proposed may aid in the systematic design of new sulfur(-II) oscillators.

Acknowledgment. One of us (Q.G.) acknowledges funding by the National Science Foundation of China (29573109) and the Science fund of CUMT (A81301).

Supporting Information Available: Figure 1S, showing the pH and mV vs Time. Figure 2S, showing simulated batch pH vs Time trace for the shortened model. Figure 3S, showing simulated CSTR pH vs time trace for changing concentrations of oxidant. This Material is available free of charge via the Internet at <http://pubs.acs.org>.

References and Notes

- (1) De Kepper, P.; Epstein, I. R.; Kustin, K. *J. Am. Chem. Soc.* **1981**, *103*, 2133.
- (2) Orbán, M.; De Kepper, P.; Epstein, I. R. *J. Phys. Chem.* **1982**, *86*, 431.
- (3) Orbán, M. *React. Kinet. Catal. Lett.* **1990**, *42*, 343.
- (4) Alamgir, M.; Epstein, I. R. *J. Phys. Chem.* **1985**, *89*, 3611.
- (5) Alamgir, M.; Epstein, I. R. *Int. J. Chem. Kinet.* **1985**, *17*, 429.
- (6) Epstein, I. R.; Kustin, K. *J. Phys. Chem.* **1985**, *89*, 2275.
- (7) Citri, O.; Epstein, I. R. *J. Phys. Chem.* **1987**, *91*, 6034.
- (8) Lengyel, I.; Rábai, G.; Epstein, I. R. *J. Am. Chem. Soc.* **1990**, *112*, 9104.
- (9) Rábai, G.; Orbán, M. *J. Phys. Chem.* **1993**, *97*, 5935.
- (10) Epstein, I. R.; Kustin, K.; Simoyi, R. H. *J. Phys. Chem.* **1992**, *96*, 5852.
- (11) Orbán, M.; Epstein, I. R. *J. Am. Chem. Soc.* **1985**, *107*, 2302.
- (12) Orbán, M. *J. Am. Chem. Soc.* **1986**, *108*, 6893.
- (13) Orbán, M.; Epstein, I. R. *J. Am. Chem. Soc.* **1987**, *109*, 101.
- (14) Kurin-Csörgei, K.; Orbán, M.; Rábai, G.; Epstein, I. R. *J. Chem. Soc., Faraday Trans.* **1996**, *92*, 2851.
- (15) Orbán, M.; Kurin-Csörgei, K.; Rábai, G.; Epstein, I. R. *Chem. Eng. Sci.* **2000**, *55*, 267.
- (16) Rábai, G.; Orbán, M.; Epstein, I. R. *J. Phys. Chem.* **1992**, *96*, 5414.
- (17) Beck, M. T.; Rábai, G. *J. Phys. Chem.* **1985**, *89*, 3907.
- (18) Rábai, G.; Beck, M. T.; Kustin, K.; Epstein, I. R. *J. Phys. Chem.* **1989**, *93*, 2853.
- (19) Epstein, I. R.; Orbán, M. *J. Am. Chem. Soc.* **1989**, *111*, 2891.
- (20) Peintler, G.; Nagypal, I.; Epstein, I. R. *J. Phys. Chem.* **1990**, *94*, 2954.
- (21) Nagypal, I.; Epstein, I. R. *J. Phys. Chem.* **1986**, *90*, 6285.
- (22) Doona, C. J.; Stanbury, D. M. *J. Phys. Chem.* **1994**, *98*, 12630.
- (23) Evans, D. F.; Upton, M. W. *J. Chem. Soc., Dalton Trans.* **1985**, *1151*, 2525.
- (24) Rábai, G.; Kustin, K.; Epstein, I. R. *J. Am. Chem. Soc.* **1989**, *111*, 3870.
- (25) Mader, P. M. *J. Am. Chem. Soc.* **1958**, *80*, 2634.
- (26) Kaps, P.; Rentrop, P. *Numer. Math.* **1979**, *33*, 55.
- (27) SIMULATE was provided courtesy of L. Gyorgi, Institute of Inorganic and Analytical Chemistry, L. Eotvos University, H-1433, Budapest, Hungary, and R. J. Field, Department of Chemistry, University of Montana, Missoula, MT 59812.
- (28) Hindmarsh, A. C. Gear: Ordinary Differential Equation Solver; Technical Report No. UCM-30001, Rev. 2; Lawrence Livermore Laboratory: Livermore, CA, 1972.
- (29) Mendes, P. *Comput. Appl. Biosci.* **1993**, *7*, 383.
- (30) Petzold, L. R. *J. Sci. Stat. Comput.* **1983**, *4*, 36.
- (31) DeKepper, P.; Epstein, I. R.; Kustin, K.; Orbán, M. *J. Phys. Chem.* **1982**, *86*, 170.
- (32) Chinake, C. R.; Simoyi, R. H. *J. Phys. Chem.* **1994**, *98*, 4012.
- (33) Chinake, C. R.; Mambo, E.; Simoyi, R. H. *J. Phys. Chem.* **1994**, *98*, 2908.
- (34) Rábai, G.; Hanazaki, I. *J. Phys. Chem. A* **1999**, *103*, 7268.